Nanoparticle-Based Test Measures Overall Propensity for Calcification in Serum

Andreas Pasch,*† Stefan Farese,*† Steffen Gräber,* Johanna Wald,‡ Walter Richtering,‡ Jürgen Floege,§ and Willi Jahnen-Dechent*

*Helmholtz Institute for Biomedical Engineering, Biointerface Laboratory, ‡Institute for Physical Chemistry, and §Department of Nephrology, Rheinisch-Westfälische Technische Hochschule (RWTH), Aachen, Germany; and †Department of Nephrology and Hypertension, University Hospital and University of Bern, Inselspital, Bern, Switzerland

ABSTRACT

Vascular and soft tissue calcification contributes to cardiovascular morbidity and mortality in both the general population and CKD. Because calcium and phosphate serum concentrations are near supersaturation, the balance of inhibitors and promoters critically influences the development of calcification. An assay that measures the overall propensity for calcification to occur in serum may have clinical use. Here, we describe a nanoparticle-based assay that detects, in the presence of artificially elevated calcium and phosphate concentrations, the spontaneous transformation of spherical colloidal primary calciprotein particles (CPPs) to elongate crystalline secondary CPPs. We used characteristics of this transition to describe the intrinsic capacity of serum to inhibit the precipitation of calcium and phosphate. Using this assay, we found that both the sera of mice deficient in fetuin-A, a serum protein that inhibits calcification, and the sera of patients on hemodialysis have reduced intrinsic properties to inhibit calcification. In summary, we developed a nanoparticle-based test that measures the overall propensity for calcification in serum. The clinical use of the test requires evaluation in a prospective study.

J Am Soc Nephrol 23: 1744–1752, 2012. doi: 10.1681/ASN.2012030240

Calcification is the final step of both physiologic and pathologic mineralization.[1] Given that calcium and phosphate concentrations are close to supersaturation and therefore, metastable in most tissues and body fluids,[2,3] calcification is imminent throughout the body. Under physiologic conditions, however, calcium and phosphate only mineralize in bones and teeth, whereas soft tissue normally does not calcify. This indicates that biomineralization is a tightly regulated, site-specific process.[1] Pathologic states perturbing this regulation lead to soft tissue and vascular calcifications, and the resulting cardiovascular diseases have become the leading cause of death and a major challenge for healthcare systems worldwide.[4,5]

We and others have identified the serum protein fetuin-A as a major systemic inhibitor of calcification.[6–9] Together with additional blood components, fetuin-A prevents the supersaturated calcium and phosphate from precipitating by forming soluble colloidal protein–mineral nanoparticles. Calcification takes place when this humoral line of defense, inherent in small molecules (particularly pyrophosphate and magnesium) and proteins (particularly fetuin-A and albumin), is overwhelmed. Accordingly, it has been shown that in the presence of fetuin-A, calcium and phosphate, even under supersaturated conditions, do not directly precipitate as crystalline hydroxyapatite [$Ca_{10}(PO_4)_6(OH)_2$]. Instead, they form soluble colloidal particles, which have been termed calciprotein particles (CPPs).[10,11] The initially formed primary CPPs spontaneously

Received March 7, 2012. Accepted June 28, 2012.

Published online ahead of print. Publication date available at www.jasn.org.

Correspondence: Dr. Andreas Pasch, Department of Nephrology and Hypertension, University Hospital and University of Bern, Inselspital, 3010 Bern, Switzerland. Email: andreas.pasch@insel.ch

convert to secondary CPPs in a transitional ripening step, which takes place in a timed and coordinated manner. This transition is associated with a change in shape and an increase in particle diameter.[11] We reasoned that this sequence of events might likewise occur in complex biological fluids and that the characteristics of this step might reflect the intrinsic inhibitory capacity of a given fluid to prevent calcium and phosphate from precipitating. We, therefore, sought to establish a reliable and clinically applicable artificial test system capable of measuring this conversion step in serum, both in a reasonable number of samples and within a reasonable time frame.

Here, we present a label-free 96-well plate-based assay, which measures the conversion of primary to secondary CPPs by detecting the time-resolved changes of laser light scattering (nephelometry) associated with it. Applying this assay, we show the impact of various variables on its performance, characterize the resulting particles, and provide data obtained with sera from humans and fetuin-A–deficient mice.

RESULTS

Test Principle

Using three-dimensional cross-correlation dynamic light scattering (3D-DLS), primary CPPs (hydrodynamic radius R_h of about 75 nm) and their spontaneous transformation to secondary CPPs (R_h of about 120 nm) were studied in an artificial solution containing fetuin-A, calcium, and phosphate (Figure 1A).[10] When calcium and phosphate solutions were mixed in the absence of fetuin-A, a coarse whitish precipitate immediately formed (Figure 1B). In contrast, when calcium and phosphate were mixed in the presence of serum, the initially clear solution turned slightly turbid within about 1 minute, and it was distinctly more turbid after about 400 minutes (Figure 1B). Given these clearly visible changes, we reasoned that this turbidity change might represent CPPs generated in the presence of human serum similar to the CPP formation previously observed in fetuin-A–containing test solutions.

When applying 3D-DLS to serum-containing solutions, the resulting readout (Figure 1C) was indeed comparable with the readout obtained with the artificial fetuin-A–containing solution (Figure 1A). Primary CPPs (R_h of about 60 nm) underwent spontaneous conversion to secondary CPPs (R_h of about 150 nm), albeit with more time lag than in simple fetuin-A solutions. Given the different transition times, we deduced that the delay of the conversion step reflected the stability of primary CPPs and that measuring this step provides an estimate of the calcification inhibitory potency inherent in serum.

Because 3D-DLS is not widely available and can measure only a single sample at a time, we aimed to establish a more practical and broadly applicable alternative assay for the detection of the transition step. Nephelometry is based on the same principles as dynamic light scattering and quantifies the amount of laser light scatter in turbid solutions (Figure 1D). Accordingly, the transition step was also detectable by time-resolved nephelometry (Figure 1E). We used an automated laser-based microplate nephelometer (Nephelostar; BMG Labtech) to analyze the primary to secondary CPP transformation in serum in 96-well plates (Figure 1F).

To this end, we analyzed precipitation times in the presence of different calcium and phosphate concentrations and the presence or absence of albumin or serum (Supplemental Figure 1). Higher temperatures accelerated precipitation, whereas serum (Supplemental Figure 1, G–I) or albumin (Supplemental Figure 1, D–F) delayed precipitation. Other than temperature, precipitation strongly depended on pH (Supplemental Figure 2A).

Given the high precipitation variability under the initially chosen conditions, the initially selected Tris buffer was exchanged for the less temperature-sensitive Hepes buffer (Supplemental Figure 2, B and C), and 10 mM calcium and 6 mM phosphate were chosen to achieve mineral ion supersaturation (Supplemental Figure 3A).

Furthermore, the addition of 140 mM NaCl abolished instabilities of the assay attributable to ionic strength fluctuations (data not shown), the use of a high precision pipetting device minimized the influence of pipetting error (Supplemental Figure 3B), and pH adjustment by the addition of a fixed amount of 10 M NaOH solution instead of individual titrations minimized pH fluctuations (Supplemental Figure 3C).

The optimized assay (Supplemental Figure 3D) contains 80 μl serum in a total assay volume of 200 μl, and it is performed at 37°C and pH 7.40 (measured at 37°C) (Supplemental Figure 3E). To allow for void volume for spiking experiments, 20 μl 140 mM NaCl was routinely included into the standard test (Supplemental Figure 3E). The solutions were mixed in the following order: 20 μl saline, 80 μl serum, 50 μl phosphate, and 50 μl calcium solution. Routine analysis of data (96 samples at 200 measurements per sample and 3 minutes apart = 600 minutes per measurement run) was performed using Excel and GraphPad prism software to yield nonlinear regression curves, allowing the determination of the one-half maximal transition time (T_{50}) and the one-half maximal relative nephelometric units (RNU_{50}) (Figure 1E).

Characterization of Particles

Centrifugation of the solutions shown in Figure 1B resulted in the pellets shown in Figure 2A. Solutions containing primary CPPs yielded a smooth and translucent pellet, whereas secondary CPPs yielded a coarse whitish pellet (Figure 2A). Scanning and transmission electron microscopy imaging showed spherical colloidal primary (Figure 2B) and elongate spindle-shaped crystalline secondary (Figure 2C) CPPs. The variability of primary CPP diameters contrasts the uniform diameters determined by 3D-DLS, and it is probably caused by the non-uniform mechanical disaggregation of pelleted primary CPPs. Primary CPPs mainly contain fetuin-A and albumin, which was shown by Coomassie blue protein stain (Figure 2D) and

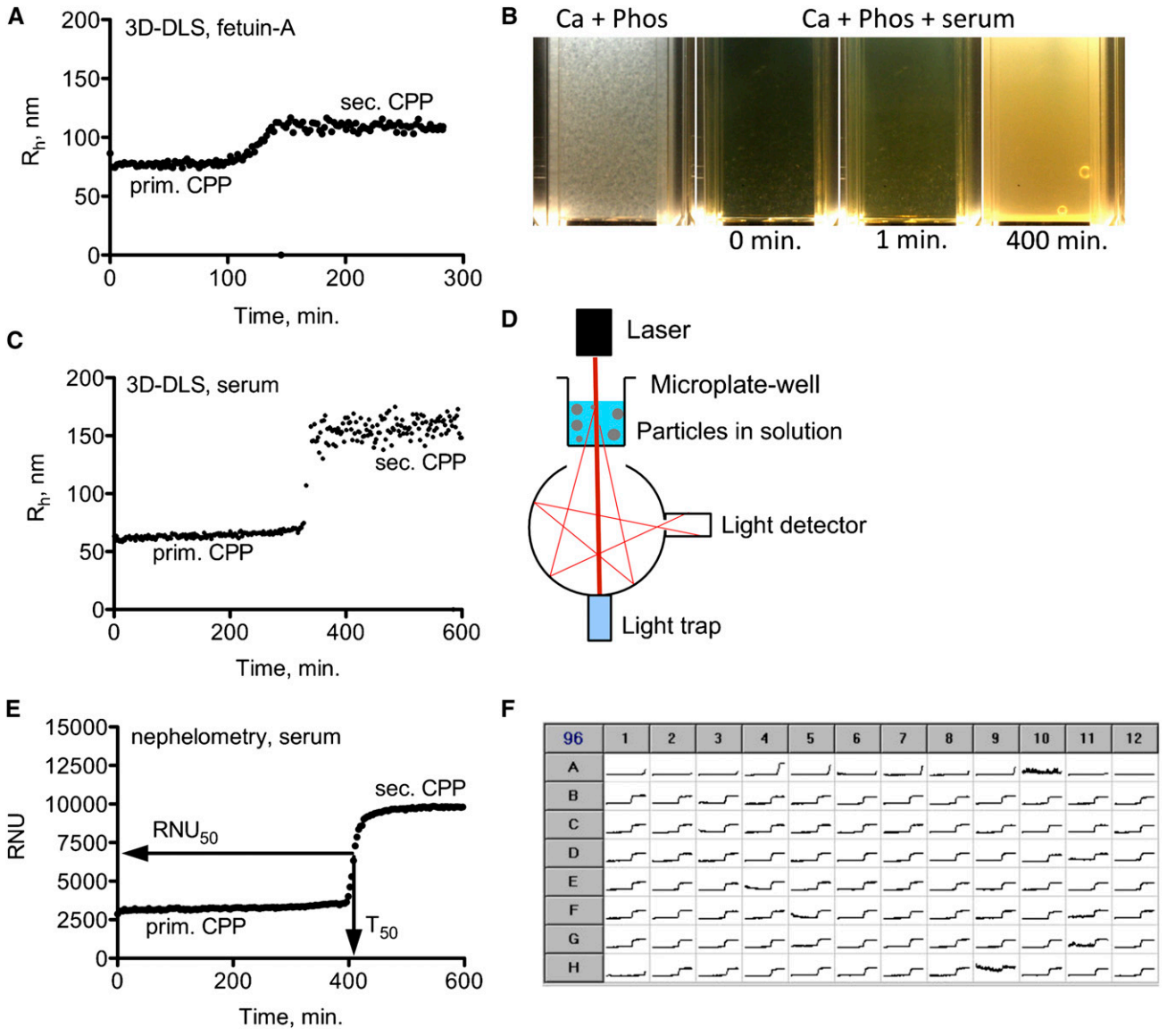

Figure 1. Test principle. (A) Three-dimensional dynamic light scattering (3D-DLS) measurement of calcium (10 mM) and phosphate (6 mM) precipitating in the presence of fetuin-A (1 g/L); primary calciprotein particles (CPPs; R_h of 75 nm) undergo spontaneous transition to secondary CPPs (R_h of 120 nm). (B) Immediate precipitation of calcium and phosphate in the absence of serum and delay of particle formation (primary and secondary CPPs) in the presence of serum; this delay reflects the intrinsic calcification-inhibitory forces of serum. (C) Precipitation of calcium and phosphate in the presence of serum monitored by 3D-DLS. (D) Schematic illustration of nephelometry, a method capable of detecting (nano) particles by measuring light scattering. (E) Nephelometric measurement of the primary to secondary CPP transformation step over time in the presence of serum. (F) Exemplary readout of serum measurements performed in 96-well plate format with the Nephelostar nephelometer (BMG Labtech). R_h, hydrodynamic radius; RNU, relative nephelometric units.

Western blot analyses (Figure 2E). In contrast, secondary CPPs comprised a more complex protein mixture. Fetuin-A and albumin were still present (Figure 2, D and E), but they did not represent the predominant components anymore. Concomitantly with the increase in pellet size (Figure 2A), phosphate concentrations in the supernatants progressively declined on formation of primary and secondary CPPs (Figure 2F).

Assay Validation

To confirm the validity of the test with regard to calcifications *in vivo*, sera from 10- to 16-month-old heavily calcified fetuin-A–deficient (−/−) and age-matched noncalcified heterozygous (+/−) and wild-type (+/+) DBA/2 mice were measured.[6] The assay discriminated the sera of these three animal groups, and the results coincided with the calcification status of the animals (Figure 3A). We also tested sera from healthy

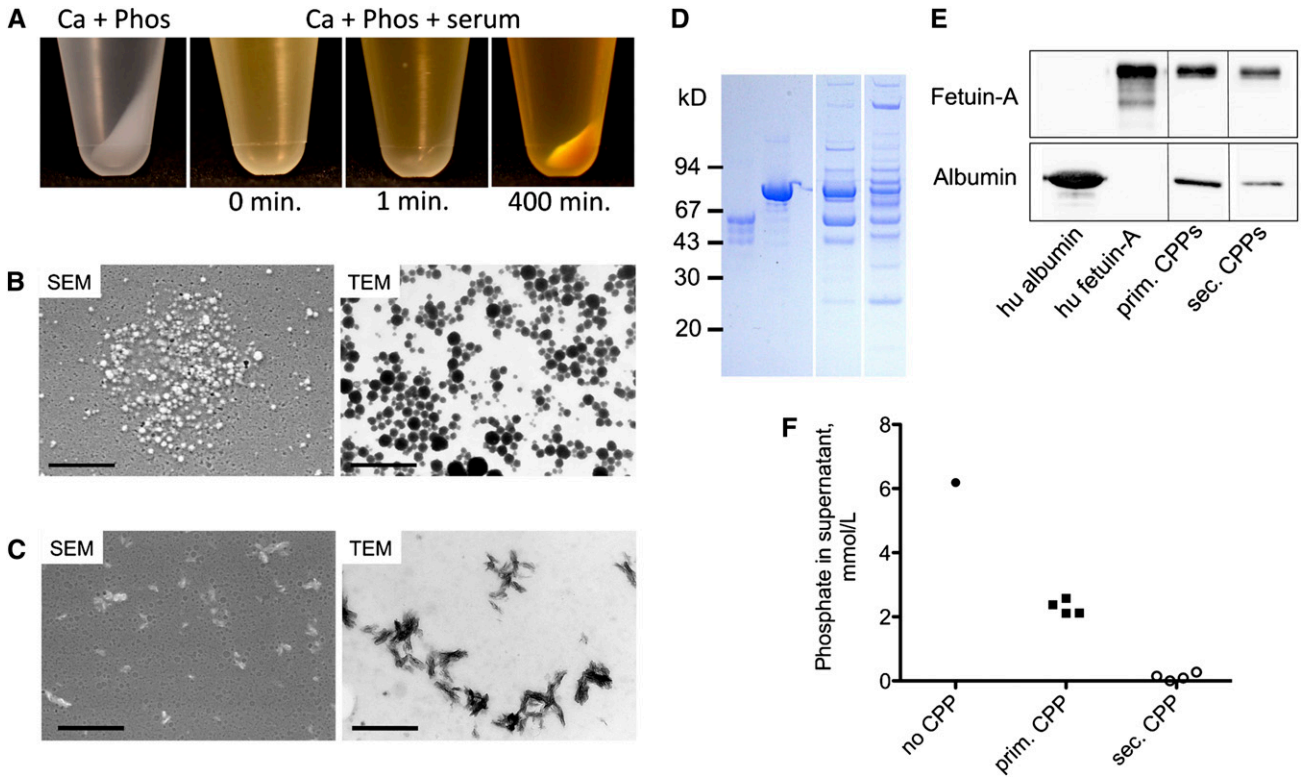

Figure 2. Particle characterization. (A) Pellets after sharp centrifugation (16,000×*g* for 120 minutes at 20°C) of the solutions shown in Figure 1A. (B) Scattering electron microscopy (SEM) and transmission electron microscopy (TEM) of primary CPPs. (C) SEM and TEM of secondary CPPs. (D) Coomassie blue stain of protein contents of primary and secondary CPPs. (E) Albumin and fetuin-A Western blots of primary and secondary CPPs. (F) Decrease of phosphate concentrations from supernatant solution on formation of primary and secondary CPPs. Scale bars, 1 μm for SEM in B and C; 500 nm for TEM in B and C.

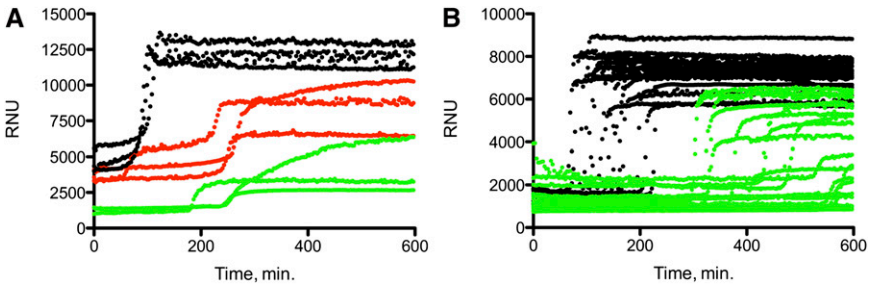

Figure 3. Serum measurements. (A) Nephelometry assay using sera from adult 10- to 16-month-old noncalcifying wild-type DBA/2 mice (green), noncalcifying heterozygous fetuin-A$^{+/-}$ knockout mice having half-normal serum fetuin-A (red), and heavily calcifying fetuin-A–deficient homozygous fetuin-A$^{-/-}$ knockout mice (black). (B) Nephelometry assay with sera from 20 hemodialysis patients (black) and 20 healthy volunteers (green).

volunteers and hemodialysis patients. Patients on hemodialysis are known to exhibit an increased risk for accelerated vascular and soft tissue calcifications.[12,13] Again, the test discriminated the calcification-prone from the noncalcification-prone individuals (*i.e.*, the hemodialysis patients from the healthy volunteers [Figure 3B]), indicating that the test reflects calcification propensity in serum.

Influence of Calcification Inhibitors and Promotors on Assay Results

Fetuin-A concentrations are known to be lower in serum of hemodialysis patients than serum from healthy individuals.[14] We, therefore, tested the impact of serum-derived proteins and small molecules[15,16] on the performance of the assay by spiking the assay with fetuin-A, albumin, lysozyme, calcium, phosphate, or magnesium. An inhibitory effect was detectable only when fetuin-A was spiked into the samples in the absence of serum (Figure 4A). In contrast, all tested compounds had a pronounced effect when they were spiked into the assay in the presence of serum (Figure 4B), with fetuin-A, albumin, and magnesium exhibiting calcification-inhibitory properties and lysozyme, phosphate, and calcium exhibiting calcification-promoting properties. The effect of calcium was relatively weak. For direct comparison, the RNU_{50} and T_{50} values from Figure 4B were combined in Figure 4C.

Fetuin-A had intrinsic precipitation-inhibiting properties (Supplemental Figure 4A), which were augmented by albumin

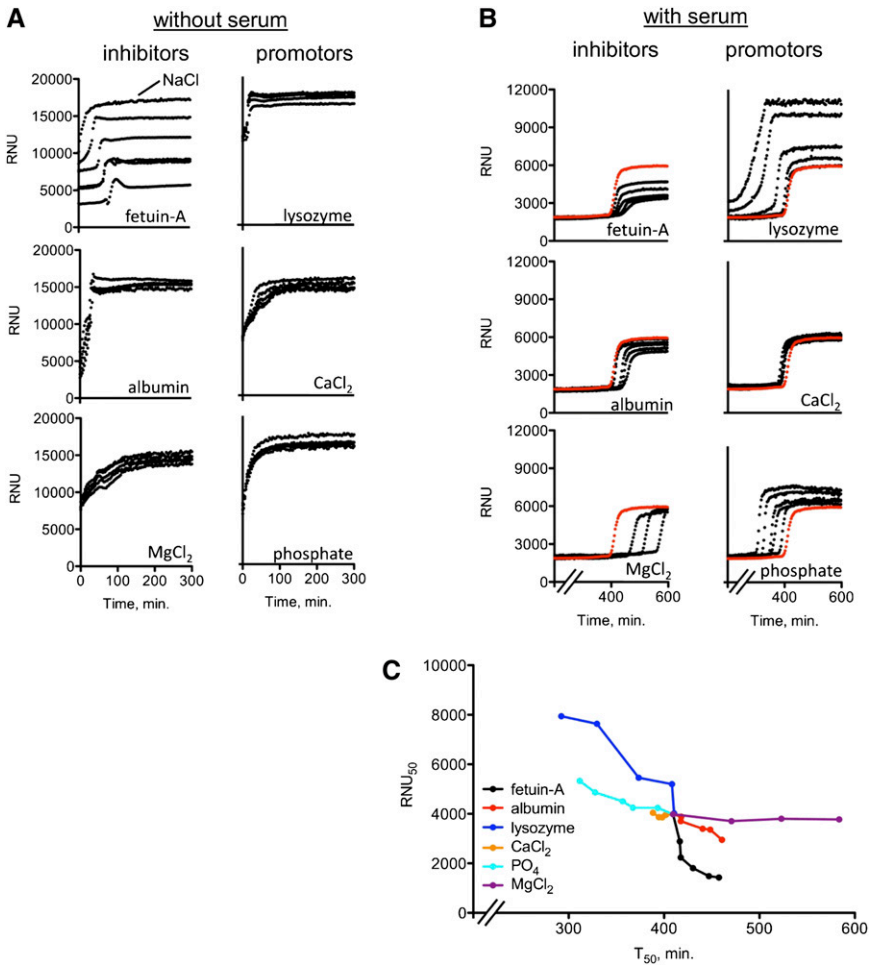

Figure 4. Impact of selected serum components on test readout. (A) Nephelometry assay in the absence of serum. Spiking with fetuin-A delayed the transition from primary to secondary CPPs. and decreased RNU. NaCl indicates a reference precipitation curve without spiking. (B) Nephelometry assay in the presence of serum. Note that fetuin-A, albumin, and magnesium inhibited and lysozyme, phosphate, and calcium promoted precipitation. The red, nonspiked reference curve is the pooled serum from healthy volunteers. (C) Alternative presentation of T_{50} and RNU_{50} values taken from Figure 4B. Minerals mainly influence T_{50}, whereas proteins influence both T_{50} and RNU_{50}. Quantities spiked in A and B: fetuin-A: 0.0625, 0.125, 0.25, 0.375, and 0.5 g/L (normal serum concentration is about 0.5 g/L); albumin: 3.125, 6.25, 12.5, 25, and 50 g/L (normal serum concentration is 35–52 g/L); lysozyme: 3.125, 6.25, 12.5, 25, and 50 g/L (normally not present in serum); Ca^{2+}: 0.25, 0.75, 1.0, 1.5, and 2.0 mmol/L (normal serum concentration is 2.1–2.55 mmol/L); PO_4: 0.25, 0.75, 1.0, 1.5, and 2.0 mmol/L (normal serum concentration is 0.84–1.45 mmol/L); Mg^{2+}: 0.25, 0.5, and 0.75 mmol/L (normal serum concentration is 0.75–1.0 mmol/L).

(Supplemental Figure 4E). In contrast, albumin had no intrinsic inhibitory effect (Supplemental Figure 4B), but the addition of increasing amounts of fetuin-A to albumin again yielded a synergistic inhibitory effect in our test (Supplemental Figure 4F). Serum fetuin-A concentrations of hemodialysis patients (Figure 3B) correlated well with the RNU_{50} ($P<0.001$) and T_{50} ($P=0.04$) values in our test (Supplemental Figure 5).

DISCUSSION

To the best of our knowledge, we present here the first potentially widely applicable technique with a reasonable throughput capacity for measuring extraosseous calcification propensity. Our test increases supersaturation of serum by adding Ca (10 mM) and phosphate (6 mM). The specific effect of supersaturation depends on the intrinsic concentrations of fetuin-A, albumin, phosphate, etc. in a given serum. As a general rule, the higher the calcium and phosphate supersaturation, the lower the T_{50} value and the higher the RNU_{50} value. This rule applies to sera from hemodialysis patients and healthy volunteers alike. RNU_{50} largely depends on the protein (fetuin-A or albumin) content of the CPPs with some contribution of phosphate. T_{50} largely depends on Mg and phosphate with some contribution of fetuin-A and albumin. A low T_{50} is, therefore, often associated with a high RNU_{50} and *vice versa*. A universal RNU_{50} to T_{50} ratio cannot, however, be determined, because both variables depend on different—albeit overlapping—determinants.

When analyzing serum obtained from fetuin-A–deficient mice or humans on hemodialysis, the test discriminates calcified (*i.e.*, fetuin-A deficient) from noncalcified mice and calcification-prone (*i.e.*, hemodialysis patients) from healthy individuals (Figure 3). These observations indicate that the test indeed quantifies the inhibitory potency of calcification.

The test principle is based on the detection of a spontaneous transitional ripening step from primary to secondary CPPs detected by time-resolved nephelometry (Figure 5). The use of supraphysiologic calcium and phosphate concentrations at physiologic temperature accelerates this process. In contrast, when occurring in the presence of lower calcium and phosphate concentrations at room temperature, CPP formation progresses only over weeks to months.[8,9,17] Under the established conditions, the 96-well format along with a measurement time of 10 hours allows the measurement of about 200 samples/d.

Calcium and phosphate readily assemble and form a crystalline precipitate in the absence of proteins (Figure 1B). This process is delayed and proceeds in a stepwise fashion in the presence of serum, a complex blend of proteins and small molecules (Figure 1, C and E). Here, as a first step, spherical

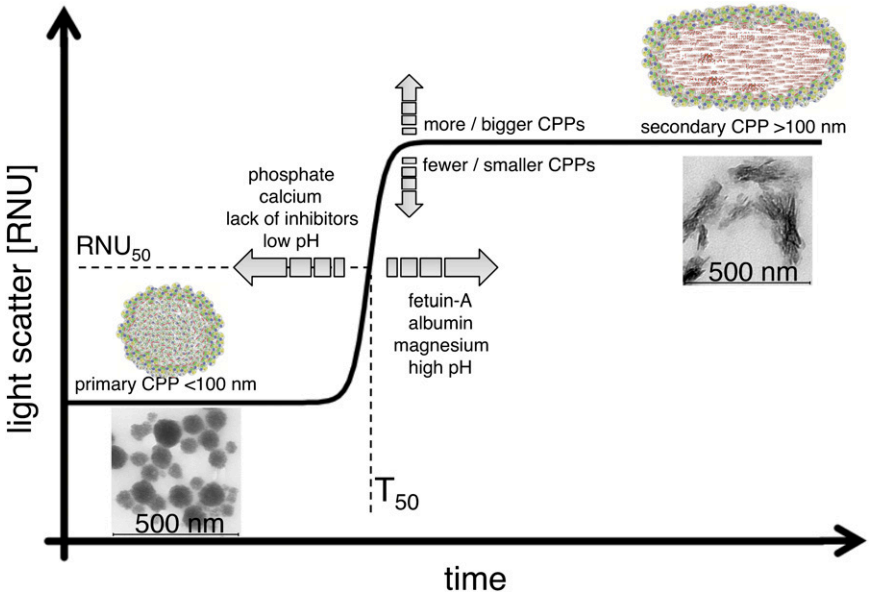

Figure 5. Schematic illustration of test principle. The addition of 10 mM calcium and 6 mM phosphate to serum triggers the formation of primary CPPs (<100 nm), reflecting a serum-intrinsic defense mechanism against calcification. Primary CPPs contain fetuin-A and albumin as well as amorphous calcium phosphate. Primary CPPs undergo spontaneous transformation into secondary CPPs, which contain crystalline calcium phosphate and an extended spectrum of serum proteins. The transformation time (T_{50}) is specific for individual sera and depends on—among other factors—the concentration of the serum constituents indicated in the figure. The transformation from primary to secondary CPPs is detected by time-resolved nephelometry and provides an estimate of the integrated calcification-inhibitory capacity present in this particular serum sample.

nanoparticles containing proteins and noncrystallized calcium and phosphate (primary CPPs) are formed that stabilize the process of calcium–phosphate precipitation in an amorphous precrystalline state (Figure 2B). As a second step, these particles undergo timely coordinated transitional ripening to elongate spindle-shaped particles (secondary CPPs), which contain proteins and crystalline calcium–phosphate (Figure 2C).

The formation of serum-derived primary CPPs in our assay depends on the presence of fetuin-A, the strongest serum-inherent calcification inhibitor, with albumin acting synergistically (Figure 4B and Supplemental Figures 4 and 5). In contrast, the timing of the primary to secondary CPP transition largely depends on the presence of small molecules, with phosphate and calcium accelerating and magnesium delaying crystallization (Figure 4, B and C). The finding that specific proteins largely define primary CPP assembly and shape, whereas small molecules largely define primary CPP stability and timing of primary to secondary CPP conversion, provides a conceptual framework of calcification regulation.

Interestingly, high concentrations of lysozyme (Figure 4, B and C) and gelatin (data not shown) disturb this ordered process of particle formation, indicating that certain proteins might act as crystallization promotors.

Of note, although alkaline pH promotes calcium–phosphate precipitation in the absence of proteins (Supplemental Figure 2A), it inhibits the transitional ripening step from primary into secondary CPPs (Supplemental Figure 3C) (*i.e.*, it stabilizes primary CPPs). This finding is in agreement with the finding of a casein fragment inhibiting calcium–phosphate precipitation in the presence of alkaline pH.[18]

CPPs occur *in vivo* in pathologic situations like CKD, which are characterized by concentration changes of proteinaceous or mineral calcification inhibitors or promotors.[19–21] In analogy, fetuin–mineral complexes were found in bisphosphonate-treated hypercalcemic rats.[22] We assume that primary CPPs are the predominant form that can be isolated from freshly drawn blood[19] and that their occurrence reflects imminent or active ongoing pathologic calcification. Reverse logic applies to our serum test: high primary and/or secondary CPP and thus, a high refractive signal and late transition times indicate a high residual capacity of the serum to form CPPs and thus, an intact humoral defense against calcification. The procalcific mileu found in dialysis patients or fetuin-A–deficient mice will exhaust this defense. Accordingly, the stability of primary CPPs—reflected by the transition time T_{50} from primary to secondary CPPs—reflects the calcification propensity both in fetuin-A–deficient mice and hemodialysis patients (Figure 3).

When trapped in body compartments, primary CPPs can undergo transition to secondary CPPs, which was shown in a case of progressive calcifying peritonitis[7,23] and cases of amputated limbs of diabetic patients.[24]

A weakness of our method is that, as a serum test, it does not by nature take into account the established contribution of cells, including vascular smooth muscle cells[25] and calcifying myeloid cells,[26] in promoting vascular calcifications *in vivo*.[27–30] Because serum represents the endogenous milieu surrounding all cells in the body, however, investigating possible CPP–cell interactions will likely also broaden our understanding of calcification processes *in vivo*.[31] Another weakness of our test is that, because of the presence of a strong buffer (50 mM Hepes), the pH present in serum does not influence the test. However, disregarding the serum-inherent bicarbonate buffer and pH allows the application of our test in a routine clinical setting with serum taken, processed, and stored under routine clinical conditions. This application, along with the 96-well format, makes our test the first potentially suitable assay for widespread use in a clinical setting.

In summary, we present a novel 96-well nephelometer-based assay, which measures calcification risk in serum. Given the relevance of calcifications for patient morbidity and mortality, it may be a useful tool for the investigation of biomineralization-related issues in both routine clinical use as well as clinical and basic research.

CONCISE METHODS

Sampling and Preparation of Serum Samples

Serum samples from venous blood were obtained from 20 hemodialysis patients and 20 healthy volunteers who had given written consent. Mouse sera from 10- to 16-week-old DBA/2 fetuin-A–deficient, heterozygous, and wild-type mice[6] were prepared by cardiac puncture at the time of sacrifice. All blood samples were clotted at room temperature for 30 minutes and spun at 2000×*g* for 10 minutes at room temperature to separate serum from blood cells. The serum was frozen and stored at −70°C until further use. For the measurements, samples were thawed at room temperature and centrifuged at 10,000×*g* for 30 minutes at room temperature to remove potential calcification nidi (cryoprecipitates).

Devices, Plastic Materials, and Chemicals

The Nephelostar nephelometer was from BMG Labtech (Offenburg, Germany), and the Liquidator96 bench-top pipetting system was from Mettler Toledo GmbH (Giessen, Germany); 96-well plates were from Brand GmbH (Wertheim, Germany), and 96-well plastic covers were from Carl Roth GmbH (Karlsruhe, Germany). All chemicals (NaCl, Tris, Hepes, $CaCl_2$, NaH_2PO_4, Na_2HPO_4, and NaOH) were purchased from AppliChem (Darmstadt, Germany) in proanalysis-grade quality. Fetal calf fetuin-A and human albumin were purchased from Sigma and Roth, respectively, and chicken egg white-derived lysozyme was purchased from Applichem; after dissolving in 140 mM NaCl, fetuin-A and lysozyme were dialyzed against a large volume of 140 mM NaCl to remove excess salt ions brought into the solutions from the protein lyophilisates. Protein concentrations were measured with the Pierce BCA Protein Assay Kit from Thermo Scientific, with bovine serum albumin as a standard.

3D-DLS

The high particle density leads to a turbidity of the investigated samples. This finding comes along with multiple scattering, which prevents particle characterization by dynamic light scattering methods. Hence, a 3D-DLS setup was used. Measurements were performed using a standard light-scattering device (ALV GmbH, Langen, Germany) with a He-Ne laser (632.8 nm, 25 mW, Type LGTC 685-35, JDS Uniphase; KOHERAS GmbH), two avalanche photodiodes (Type SPCM-AQR-13-FC; Perkin Elmer), and an ALV 7002 correlator. The scattered light was detected at 90° geometry. Temperature control was ensured by using an external thermostat equipped with a Pt-100 temperature sensor. The hydrodynamic radius R_h was calculated from second-order cumulant fits by the Stokes–Einstein equation. Measurements were performed in 2-minute intervals.

Nephelometer Assay

Stock solution 1 was NaCl solution: 140 mM NaCl. Stock solution 2 was calcium solution: 40 mM $CaCl_2$+100 mM Hepes+140 mM NaCl pH-adjusted with 10 M NaOH to 7.40 at 37°C. Stock solution 3 was phosphate solution: 19.44 mM Na_2HPO_4+4.56 mM NaH_2PO_4+100 mM Hepes+140 mM NaCl pH-adjusted with 10 M NaOH to 7.40 at 37°C. For preparation of 96-well plates, all solutions were prewarmed to 34.5°C in a thermoconstant room, where all pipetting steps were performed with the Liquidator96 bench-top pipetting system using a set of new pipetting tips for every pipetting step. These pipetting steps were performed in the following order: (*1*) NaCl solution: 20 μl/well, (*2*) serum: 80 μl/well, (*3*) shaking for 1 minute, (*4*) phosphate solution: 50 μl/well, (*5*) shaking for 1 minute, and (*6*) calcium solution: 50 μl/well and shaking for 1 minute. Air bubbles in the wells were disintegrated with a pocket lighter, and the 96 wells were covered with a ThinSeal adhesive sealing film for microplates. Because line A of the 96-well plate often showed unreliable results, it was generally not used (compare with Figure 1F). Assay conditions and Nephelostar settings were measurement in a thermoconstant room at 34.5°C with the internal radiation of the Nephelostar device turned off. This led to an internal measurement temperature of 36.5°C to 37°C. The Nephelostar was operated and controlled through the Nephelostar provider's Galaxy software on a Windows computer platform. The assay was performed for 200 cycles with 1.5-seconds measurement time per well and a position delay of 0.1 seconds in horizontal plate reading mode, adding up to a cycle time of 180 seconds per cycle for our standard assay. This assay adds up to a total assay run time of 10 hours per assay. For some measurements, the cycle time was extended to 360 or 540 seconds, which adds up to assay times of 20 and 30 hours, respectively. The gain and laser adjustment was set at 90% required value, gain 50 with a laser beam focus of 1.5 mm, and laser intensity of 50%. After completion of the run, data were transferred to Excel and transposed from lines into columns. Data columns were copied into the GraphPad Prism program to generate an XY graph. Data were then processed by calculating nonlinear regression in the log(agonist) vs. response–variable slope (four parameters) mode using the robust fit fitting method. The resulting values obtained for T_{50} and RNU_{50} were further processed as required.

Protein Detection and Quantification Methods

For quantification of proteins in solutions, the Pierce BCA Protein Assay Kit was used according to the manufacturer's instructions. BSA (2 mg/ml; Pierce) was used as a standard. Western blots were performed according to standard protocols with SDS-PAGE (4%–12%), with 1 μg protein or 0.4 μg pure fetuin-A or albumin loaded per lane. The following primary antibodies against fetuin-A and albumin were used: polyclonal rabbit anti-human fetuin-A antiserum 5359 (H. Haupt, Bering) and mouse anti-human albumin (1:2500, catalog number 0300–0080; AbD Serotec). For fluorescence detection, the following horseradish peroxidase-coupled secondary antibodies were used: swine anti-rabbit IgG (1:5000, catalog number P0217; Dako) and rabbit anti-mouse IgG (1:2000, catalog number P0260; Dako). Protein stains were performed with the Imperial Protein Stain according to the manufacturer's instructions (Thermo Scientific); 6.0 μg total protein or 2.5 μg pure fetuin-A or albumin was loaded per lane.

Electron Microscopy

Primary and secondary CPPs were prepared at room temperature as described in Nephelometer Assay.

For transmission electron microscopy, 10 μl samples were applied onto Formvar (polyvinyl formal) -coated nickel grids (Plano, Wetzlar, Germany). The grids were dried at room temperature, and the CPPs were visualized without staining. For scanning electron microscopy, 10-μl samples were applied onto slides, dried at room temperature, coated with gold (7 nm), and visualized using a Philips XL.

ACKNOWLEDGMENTS

A.P. was supported by a personal grant from the European Renal Association—European Dialysis and Transplantation Association. Parts of this project were supported by the excellence initiative of the German federal and state governments.

DISCLOSURES

None.

REFERENCES

1. Jahnen-Dechent W, Heiss A, Schäfer C, Ketteler M: Fetuin-A regulation of calcified matrix metabolism. *Circ Res* 108: 1494–1509, 2011
2. Sandin K, Hegbrant J, Kloo L: A theoretical investigation of the supersaturation of basic calcium phosphate in serum of dialysis patients. *J Appl Biomater Biomech* 4: 80–86, 2006
3. Thurgood LA, Ryall RL: Proteomic analysis of proteins selectively associated with hydroxyapatite, brushite, and uric acid crystals precipitated from human urine. *J Proteome Res* 9: 5402–5412, 2010
4. Yusuf S, Reddy S, Ounpuu S, Anand S: Global burden of cardiovascular diseases: Part I: General considerations, the epidemiologic transition, risk factors, and impact of urbanization. *Circulation* 104: 2746–2753, 2001
5. Blacher J, Guerin AP, Pannier B, Marchais SJ, London GM: Arterial calcifications, arterial stiffness, and cardiovascular risk in end-stage renal disease. *Hypertension* 38: 938–942, 2001
6. Schafer C, Heiss A, Schwarz A, Westenfeld R, Ketteler M, Floege J, Muller-Esterl W, Schinke T, Jahnen-Dechent W: The serum protein alpha 2-Heremans-Schmid glycoprotein/fetuin-A is a systemically acting inhibitor of ectopic calcification. *J Clin Invest* 112: 357–366, 2003
7. Heiss A, Eckert T, Aretz A, Richtering W, van Dorp W, Schäfer C, Jahnen-Dechent W: Hierarchical role of fetuin-A and acidic serum proteins in the formation and stabilization of calcium phosphate particles. *J Biol Chem* 283: 14815–14825, 2008
8. Young JD, Martel J, Young D, Young A, Hung CM, Young L, Chao YJ, Young J, Wu CY: Characterization of granulations of calcium and apatite in serum as pleomorphic mineralo-protein complexes and as precursors of putative nanobacteria. *PLoS One* 4: e5421, 2009
9. Young JD, Martel J, Young L, Wu CY, Young A, Young D: Putative nanobacteria represent physiological remnants and culture by-products of normal calcium homeostasis. *PLoS One* 4: e4417, 2009
10. Heiss A, DuChesne A, Denecke B, Grötzinger J, Yamamoto K, Renné T, Jahnen-Dechent W: Structural basis of calcification inhibition by alpha 2-HS glycoprotein/fetuin-A. Formation of colloidal calciprotein particles. *J Biol Chem* 278: 13333–13341, 2003
11. Wald J, Wiese S, Eckert T, Jahnen-Dechent W, Richtering W, Heiss A: Formation and stability kinetics of calcium phosphate–fetuin-A colloidal particles probed by time-resolved dynamic light scattering. *Soft Matter* 7: 2869–2874, 2011
12. Goodman WG, Goldin J, Kuizon BD, Yoon C, Gales B, Sider D, Wang Y, Chung J, Emerick A, Greaser L, Elashoff RM, Salusky IB: Coronary-artery calcification in young adults with end-stage renal disease who are undergoing dialysis. *N Engl J Med* 342: 1478–1483, 2000
13. Oh J, Wunsch R, Turzer M, Bahner M, Raggi P, Querfeld U, Mehls O, Schaefer F: Advanced coronary and carotid arteriopathy in young adults with childhood-onset chronic renal failure. *Circulation* 106: 100–105, 2002
14. Ketteler M, Bongartz P, Westenfeld R, Wildberger JE, Mahnken AH, Böhm R, Metzger T, Wanner C, Jahnen-Dechent W, Floege J: Association of low fetuin-A (AHSG) concentrations in serum with cardiovascular mortality in patients on dialysis: A cross-sectional study. *Lancet* 361: 827–833, 2003
15. Wilson JW, Werness PG, Smith LH: Inhibitors of crystal growth of hydroxyapatite: A constant composition approach. *J Urol* 134: 1255–1258, 1985
16. Schlieper G, Westenfeld R, Brandenburg V, Ketteler M: Inhibitors of calcification in blood and urine. *Semin Dial* 20: 113–121, 2007
17. Wu CY, Martel J, Young D, Young JD: Fetuin-A/albumin-mineral complexes resembling serum calcium granules and putative nanobacteria: Demonstration of a dual inhibition-seeding concept. *PLoS One* 4: e8058, 2009
18. Reeves RE, Latour NG: Calcium phosphate sequestering phosphopeptide from casein. *Science* 128: 472, 1958
19. Fraikin JL, Teesalu T, McKenney CM, Ruoslahti E, Cleland AN: A high-throughput label-free nanoparticle analyser. *Nat Nanotechnol* 6: 308–313, 2011
20. Smith ER, Ford ML, Tomlinson LA, Rajkumar C, McMahon LP, Holt SG: Phosphorylated fetuin-A-containing calciprotein particles are associated with aortic stiffness and a procalcific milieu in patients with predialysis CKD. *Nephrol Dial Transplant* 27: 1957–1966, 2012
21. Hamano T, Matsui I, Mikami S, Tomida K, Fujii N, Imai E, Rakugi H, Isaka Y: Fetuin-mineral complex reflects extraosseous calcification stress in CKD. *J Am Soc Nephrol* 21: 1998–2007, 2010
22. Price PA, Nguyen TM, Williamson MK: Biochemical characterization of the serum fetuin-mineral complex. *J Biol Chem* 278: 22153–22160, 2003
23. Olde Loohuis KM, Jahnen-Dechent W, van Dorp W: The case: Milky ascites is not always chylous. *Kidney Int* 77: 77–78, 2010
24. Ghadially FN: As you like it, Part 3: A critique and historical review of calcification as seen with the electron microscope. *Ultrastruct Pathol* 25: 243–267, 2001
25. Byon CH, Sun Y, Chen J, Yuan K, Mao X, Heath JM, Anderson PG, Tintut Y, Demer LL, Wang D, Chen Y: Runx2-upregulated receptor activator of nuclear factor κB ligand in calcifying smooth muscle cells promotes migration and osteoclastic differentiation of macrophages. *Arterioscler Thromb Vasc Biol* 31: 1387–1396, 2011
26. Fadini GP, Albiero M, Menegazzo L, Boscaro E, Vigili de Kreutzenberg S, Agostini C, Cabrelle A, Binotto G, Rattazzi M, Bertacco E, Bertorelle R, Biasini L, Mion M, Plebani M, Ceolotto G, Angelini A, Castellani C, Menegolo M, Grego F, Dimmeler S, Seeger F, Zeiher A, Tiengo A, Avogaro A: Widespread increase in myeloid calcifying cells contributes to ectopic vascular calcification in type 2 diabetes. *Circ Res* 108: 1112–1121, 2011
27. Reynolds JL, Skepper JN, McNair R, Kasama T, Gupta K, Weissberg PL, Jahnen-Dechent W, Shanahan CM: Multifunctional roles for serum protein fetuin-a in inhibition of human vascular smooth muscle cell calcification. *J Am Soc Nephrol* 16: 2920–2930, 2005
28. Reynolds JL, Joannides AJ, Skepper JN, McNair R, Schurgers LJ, Proudfoot D, Jahnen-Dechent W, Weissberg PL, Shanahan CM: Human vascular smooth muscle cells undergo vesicle-mediated calcification in

response to changes in extracellular calcium and phosphate concentrations: A potential mechanism for accelerated vascular calcification in ESRD. *J Am Soc Nephrol* 15: 2857–2867, 2004
29. Speer MY, Yang HY, Brabb T, Leaf E, Look A, Lin WL, Frutkin A, Dichek D, Giachelli CM: Smooth muscle cells give rise to osteochondrogenic precursors and chondrocytes in calcifying arteries. *Circ Res* 104: 733–741, 2009
30. Pasch A, Schaffner T, Huynh-Do U, Frey BM, Frey FJ, Farese S: Sodium thiosulfate prevents vascular calcifications in uremic rats. *Kidney Int* 74: 1444–1453, 2008
31. Chen NX, O'Neill KD, Chen X, Duan D, Wang E, Sturek MS, Edwards JM, Moe SM: Fetuin-A uptake in bovine vascular smooth muscle cells is calcium dependent and mediated by annexins. *Am J Physiol Renal Physiol* 292: F599–F606, 2007

This article contains supplemental material online at http://jasn.asnjournals.org/lookup/suppl/doi:10.1681/ASN.2012030240/-/DCSupplemental.